Published in final edited form as:
Nucl Med Biol. 2008 April ; 35(3): 263–272. doi:10.1016/j.nucmedbio.2007.11.007.

$^{99m}Tc(CO)_3$-DTMA bombesin conjugates having high affinity for the GRP receptor

Stephanie R. Lane[b,f], **Bhadrasetty Veerendra**[a], **Tammy L. Rold**[e], **Gary L. Sieckman**[b], **Timothy J. Hoffman**[b,d,f], **Silvia S. Jurisson**[f], and **Charles J. Smith**[a,b,c,d,*]

[a]Department of Radiology, University of Missouri-Columbia School of Medicine, Columbia, MO 65211, USA

[b]Research Division, Harry S. Truman Memorial Veterans' Hospital, Columbia, MO 65201, USA

[c]University of Missouri Research Reactor Center, University of Missouri-Columbia, Columbia, MO 65211, USA

[d]The Radiopharmaceutical Sciences Institute, University of Missouri-Columbia School of Medicine, Columbia, MO 65211, USA

[e]Department of Internal Medicine, University of Missouri-Columbia School of Medicine, Columbia, MO 65211, USA

[f]Department of Chemistry, University of Missouri-Columbia, Columbia, MO 65211, USA

Abstract

Introduction—Targeted diagnosis of specific human cancer types continues to be of significant interest in nuclear medicine. ^{99m}Tc is ideally suited as a diagnostic radiometal for in vivo tumor targeting due to its ideal physical characteristics and diverse labeling chemistries in numerous oxidation states.

Methods—In this study, we report a synthetic approach toward design of a new tridentate amine ligand for the organometallic aqua-ion $[^{99m}Tc(H_2O)_3(CO)_3]^+$. The new chelating ligand framework, 2-(*N*,*N*′-Bis(*tert*-butoxycarbonyl)diethylenetriamine) acetic acid (DTMA), was synthesized from a diethylenetriamine precursor and fully characterized by mass spectrometry and nuclear magnetic resonance spectroscopy (^1H and ^{13}C). DTMA was conjugated to H_2N-(X)-BBN(7–14)NH_2, where *X*=an amino acid or aliphatic pharmacokinetic modifier and BBN=bombesin peptide, by means of solid phase peptide synthesis. DTMA-(X)-BBN(7–14)NH_2 conjugates were purified by reversed-phase high-performance chromatography and characterized by electrospray-ionization mass spectrometry.

Results—The new conjugates were radiolabeled with $[^{99m}Tc(H_2O)_3(CO)_3]^+$ produced via Isolink radiolabeling kits to produce $[^{99m}Tc(CO)_3$-DTMA-(X)-BBN(7–14)$NH_2]$. Radiolabeled conjugates were purified by reversed-phase high-performance chromatography. Effective receptor binding behavior was evaluated in vitro and in vivo.

Conclusions—$[^{99m}Tc(CO)_3$-DTMA-(X)-BBN(7–14)$NH_2]$ conjugates displayed very high affinity for the gastrin releasing peptide receptor in vitro and in vivo. Therefore, these conjugates hold some propensity to be investigated as molecular imaging agents that specifically target human cancers uniquely expressing the gastrin releasing peptide receptor subtypes.

*Corresponding author. Harry S. Truman Memorial VA Hospital, Columbia, MO 65201, USA. Tel.: +1 573 814 6000x3683; fax: +1 573 882 1663. *E-mail address:* E-mail: smithcj@health.missouri.edu (C.J. Smith).

Keywords

Bombesin; Prostate; Tridentate; Tricarbonyl; Internalization; Biodistribution

1. Introduction

Bombesin peptide (BBN) is a 14-amino acid analog of human gastrin releasing peptide (GRP) originally isolated from the skin of the frog *Bombina bombina* in 1970 [1]. There are four known receptor subtypes of BBN, including the neuromedin B receptor (subtype 1), the GRP receptor (GRPr, subtype 2), the orphan receptor (subtype 3) and the BBN receptor (subtype 4) [2]. In recent years, our group and others have focused upon development of site-directed molecular imaging agents targeting human cancers expressing the GRPr subtype [3–9]. These studies have been based primarily upon reports that specific human tumors tend to express the GRPr in very high numbers, therefore providing an approach to selectively target GRP receptor-expressing neoplasms with minimal accumulation in nontarget collateral tissue [1,2, 10–12].

The use of radiolabeled BBN targeting vectors to selectively target receptor-expressing tumors offers innovative diagnostic and treatment strategies for patients suffering from specific human cancers such as breast or prostate [1,2,10,11]. The utility to effectively image prostate and breast cancer tumor xenografts via site-directed single photon emission computed tomography (SPECT) or positron emission tomography (PET) using ^{111}In- or ^{64}Cu-radiolabeled BBN molecular imaging agents provides impetus toward further development of new molecular imaging strategies in order to overcome the limitations of current procedures for diagnosis, staging and restaging of the disease. ^{99m}Tc is a versatile radiometal for use in molecular imaging of human tumors due to its ideal physical properties ($t_{½}$=6 h and 140 keV gamma emission), onsite availability from a ^{99}Mo/^{99m}Tc generator and diverse labeling chemistry [13–15]. ^{99m}Tc has proven its utility in nuclear medicine by its use in ~85% of all diagnostic procedures in clinical nuclear medicine [16].

Organometallic, tricarbonyl, technetium chemistry has become a focus for future ^{99m}Tc radiopharmaceuticals due to the ease of reducing generator pertechnetate eluent from a 7+ oxidation state to a kinetically-inert, d^6, 1+ oxidation state via an Isolink radiolabeling kit [14,17,18]. The development of the aqua ion complex, $[^{99m}Tc(H_2O)_3(CO)_3]^+$, has generated interest for new chelating ligand frameworks that can stabilize the cationic Tc(I) metal center under *in vivo* conditions [13,17,19]. Studies have shown bi- and tridentate ligands that are composed of primary, secondary and aromatic amines to be effective chelators for the low-valent metal center, providing the stability necessary for in vivo molecular imaging of human tumor tissue [3,18,20–24]. Amines are relatively soft donor atoms and are known to have high affinity for soft acceptors [25], hence the strong binding and kinetic inertness of ^{99m}Tc-conjugates based upon these ligand frameworks. The effectiveness of using bidentate ligands for imaging of GRP receptor-expressing prostate tumors has been demonstrated by the high-quality microSPECT images obtained by Prasanphanich et al. [25,26]. Tridentate ligand frameworks, however, occupy all three binding sites on the *fac*-$[^{99m}Tc(CO)_3]^+$ metal fragment, alleviating the possibility for *trans*-metallation reactions in the presence of serum proteins and nontarget accumulation of tracer in tissue, thus offering the possibility of higher-contrast, higher-quality SPECT images.

Herein, we report the synthesis of the tridentate 2-(*N*,*N*′-Bis(*tert*-butoxycarbonyl) diethylenetriamine) acetic acid (DTMA) ligand and its conjugation to the N-terminal primary amine of H_2N-(X)-BBN(7–14)NH_2 to produce DTMA-(X)-BBN(7–14)NH_2. The BBN analog BBN(7–14) NH_2 was used in this study due to its compact size and similar homology to

mammalian GRP in the amidated C-terminal region of the peptide. GRP and BBN share an amidated C-terminus with an identical sequence homology of the seven terminal amino acids, W-A-V-G-*H*-L-M-NH_2. All of the conjugates were synthesized by solid phase peptide synthesis (SPPS) and fully characterized by negative ion electrospray-ionization mass spectrometry (ESI-MS). The conjugates were radiolabeled with $[^{99m}Tc(H_2O)_3\ (CO)_3]^+$, synthesized via an Isolink radiolabeling kit, to produce $[^{99m}Tc(CO)_3$-DTMA-(X)-BBN(7–14) $NH_2]$ conjugates in high yield. Internalization and externalization studies and competitive displacement binding assays [inhibitory concentration at 50% (IC_{50})] were performed in PC-3 human prostate cancer cells, a cell line that expresses the GRPr in very high numbers (2.7 $\pm 0.6\times 10^5$ receptors per cell) [26]. The pharmacokinetics of the series of $[^{99m}Tc(CO)_3$-DTMA-(X)-BBN(7–14)$NH_2]$ conjugates were determined in CF-1 normal mice. The $[^{99m}Tc(CO)_3$-DTMA-(β-Ala)-BBN (7–14)$NH_2]^+$ conjugate, which showed favorable uptake and retention of tracer in vitro and in normal mouse models, was evaluated in SCID mice bearing PC-3 xenografted tumors.

2. Materials and methods

2.1. Synthesis of N,N′-Bis(tert-butoxycarbonyl) diethylenetriamine

All chemicals were purchased from Aldrich Chemical (St. Louis, MO, USA) and used without further purification. American Chemical Society-certified solvents were purchased from Fisher Scientific (Pittsburgh, PA, USA) and used without further purification. 2-(tert-butoxycarbonyloxyimino)-2-(phenlacetonitrile) (BOC-ON) (4.46 g, 18.1 mmol) dissolved in tetrahydrofuran (THF) (250 ml) was slowly added dropwise to diethylenetriamine (0.933 g, 9.04 mmol) in THF (10 ml) at <0°C [ice, NaCl and $(CH_3)_2CO$]. The reaction mixture was stirred overnight, after which, solvent was removed under reduced pressure. Ligand precursor was purified by column chromatography. Methylene chloride (600 ml) was used to remove reaction byproducts, followed by 98.5% CH_2Cl_2/1.5% MeOH (600 ml) and then 100% MeOH (1000 ml). Thin layer chromatography (TLC) ran in 98.5% CH_2Cl_2/1.5% MeOH, was used to determine the progress of the separation. MeOH fractions were collected from the column and solvent was removed in vacuo to give a yellow oil (5.38 g, 98%). **^{1}H NMR** [$CDCl_3$, 500 MHz, RT, δ(ppm)] ((-O-C-**CH_3**)$_3$, s, 18H) 1.409, (-NH-**CH_2**-CH_2-NH-CH_2-**CH_2**-NH-, t, 4H) 2.675, (-NH-CH_2-**CH_2**-NH-**CH_2**-CH_2-NH-, m, 4H) 3.169, (-CO-**NH**-CH_2-CH_2-NH-, s) 5.083. **^{13}C NMR** [$CDCl_3$, 500 MHz, RT, δ(ppm)] ((-O-C-**CH_3**)$_3$) 28.31, (-NH-**CH_2**-CH_2-NH-CH_2-**CH_2**-NH-) 40.16, (-NH-CH_2-**CH_2**-NH-CH_2-CH_2-NH-) 48.70, (-**C**-$(CH_3)_3$) 79.03, (-**COO**-C-$(CH_3)_3$) 156.10. Mass spectrum [high-resolution fast atom bombardment mass spectrometry (**HR-FAB MS**)]: Anal Calc. for $C_{14}H_{29}N_3O_4$ ($M+Li^+$): 311.2346. Found: 311.2357.

2.2. Synthesis of N,N′-Bis(tert-butoxycarbonyl) diethylenetriamine ethylbromoester

BOC-DTMA (2.29 g, 7.41 mmol) was dissolved in MeCN (35 ml). To this solution was added ethylbromoacetate (1.025 ml), potassium iodide (KI) (1.51 g, 9.10 mmol) and triethylamine (5 ml). The solution was refluxed for 48 h. The orange-cream colored solution was filtered through filter paper to remove excess salt and was washed with MeCN. Removal of solvent under reduced pressure afforded the product as a clear yellow oil (2.79 g, 95%). **^{1}H NMR** [$CDCl_3$, 500 MHz, RT, δ(ppm)] (-COO-CH_2-**CH_3**, N, 3H) 1.174, (-COO-C-(**CH_3**)$_3$, s, 18H) 1.351, (-NH-**CH_2**-CH_2-N-CH_2+CH_2-NH-, t, 4H) 2.623, (-NH-CH_2-**CH_2**-N-**CH_2**-CH_2-NH-, m, 4H) 3.052, (-N-**CH_2**-COO-CH_2-CH_3, s, 2H) 3.259, (-COO-**CH_2**-CH_3, q, 2H) 4.069, (-**NH**-CH_2-CH_2-N-CH_2-CH_2-**NH**-, s, 2H) 5.180. **^{13}C NMR** [$CDCl_3$, 250 MHz, RT, δ(ppm)] (-COO-CH_2-**CH_3**) 14.05, (-COO-(**CH_3**)$_3$) 28.28, (-NH-**CH_2**-CH_2-N-CH_2-**CH_2**-NH-) 38.45, (-NH-CH_2-**CH_2**-N-**CH_2**-CH_2-NH-) 53.99, (-COO-**CH_2**-CH_3) 55.08, (-N-**CH_2**-COO-CH_2-CH_3) 60.51, (-COO-**C**-$(CH_3)_3$) 78.88, (-**COO**-C-$(CH_3)_3$) 156.04, (-**COO**-CH_2-CH_3) 171.56). **Mass spectrum (ESI-MS)**: Anal Calc. for $C_{18}H_{36}N_3O_6$ (M^+): 390.26. Found: 390.1.

2.3. Synthesis of DTMA

To BOC-DTMA-ester (2.50 g, 6.42 mmol) in MeOH (15 ml) was added 10% NaOH solution (~8 ml) until the final pH of the solution was adjusted to 11. The solution was stirred for 3 h and dried under reduced pressure. The product was dissolved in water (10 ml). A saturated solution of citric acid was added to the dissolved product until a pH of 5 was obtained. Ethyl acetate (40 ml) was added to the solution while stirring. The aqueous and organic solutions were separated via separatory funnel. The ethyl acetate layer was washed with water a total of three times and dried over sodium sulfate. The organic layer was dried in vacuo to afford a white solid. The product was washed with diethyl ether and centrifuged. The supernatant was decanted, and the white powder was dried overnight under reduced pressure (0.63 g, 27%). ^{1}**H NMR** [MeOD, 500 MHz, RT, δ(ppm)] (-COO-C-(**C**H_3)$_3$, s, 18H) 1.360, (-NH-**C**H_2-CH_2-N-CH_2-**C**H_2-NH-, m, 4H) 3.149, (-NH-CH_2-**C**H_2-N-**C**H_2-CH_2-NH-, m, 4H) 3.288, (-N-**C**H_2- COOH, s, 2H) 3.575. ^{13}**C NMR** [MeOD, 500 MHz, RT, δ(ppm)] (-COO-(**C**H_3)$_3$) 28.28, (-NH-**C**H_2-CH_2-N-CH_2-**C**H_2-NH-) 37.22, (-NH-CH_2-**C**H_2-N-**C**H_2-CH_2-NH-) 56.15, (-N-**C**H_2-COOH) 57.81, (-COO-C-(CH_3)$_3$) 80.84, (-**COO**-C-(CH_3)$_3$) 158.75, (-**COOH**) 170.81. **Mass spectrum (ESI-MS)**: Anal Calc. for $C_{16}H_{31}N_3O_6$ (M^++Li): 368.24. **Found:** 368.2.

2.4. Synthesis of DTMA-(X)-BBN(7–14)NH_2 peptide conjugates

DTMA-(X)-BBN(7–14)NH_2 conjugates were synthesized on a Perkin-Elmer-Applied Biosystem model 432A automated peptide synthesizer employing traditional Fmoc chemistry, where X denotes the linker (GGG (glycylglycylglycine), GSG (glyclylserylglycine), SSS (serylserlyserine) or β-Ala [Beta Alanine]) and BBN(7–14)NH_2 denotes the amino acid sequence, Q-W-A-V-G-H-L-M-NH_2. Rink Amide MBHA resin (25 μmol), Fmoc-protected amino acids (75 μmol) and DTMA (75 μmol) were utilized for SPPS. A cocktail of thioanisol, water, ethanedithiol and trifluoracetic acid in a ratio of 2:1:1:36 was used to cleave the peptide from the resin, followed by peptide precipitation in methyl-*t*-butyl ether. Crude peptide conjugates were obtained in 80–85% yield. The crude peptide-conjugates were purified by reversed-phase high-performance liquid chromatography (RP-HPLC), and solvents were removed in vacuo using a SpeedVac concentrator (Labconco, Kansas City, MO, USA). Negative ion mode ESI-MS was used to compare calculated to experimental molecular ion peaks. The calculated and experimental masses for the DTMA-(X)-BBN(7–14)NH_2 conjugates were as follows: X=GGG (1255.7, 1254.4), X=GSG (1285.6, 1284.9), X=SSS (1345.5, 1344.7) and X=β-Ala (1153.6, 1152.7).

2.5. RP-HPLC analyses of metallated and nonmetallated DTMA-(X)-BBN(7–14)NH_2 conjugates

RP-HPLC analyses of radiolabeled and nonradiolabeled compounds were performed on a Shimadzu SCL-10A system equipped with a Shimadzu SPD-10A UV-Vis tunable absorbance detector (set at λ=280 nm), an Eppendorf TC-50 column heater and a radiometric in-line EG&G ORTEC NaI solid scintillation detector. HPLC grade solvents were purchased from Fisher Scientific. Purification of nonmetallated conjugates was performed on a semipreparative reversed-phase C-18 column (Phenomenex Jupiter Proteo, 250×10.00 mm, 10 μm). Radiolabeling investigations were performed using an analytical reverse-phase C-18 column (Phenomenex Jupiter Proteo, 250×4.60 mm, 5 μm). The solvent system was H_2O/0.1% TFA (A) and CH_3CN/0.1% TFA (B). The gradient system began at 95% A and 5% B. From 0 to 25 min, the solvent increased linearly to 30% A and 70% B. From 25 to 30 min, the solvent increased to 5% A and 95% B.

2.6. ESI- and HR-FAB MS

HR-FAB MS analyses of the nonconjugated ligand and ligand intermediates were performed by the Washington University Mass Spectrometry Resource (St. Louis, MO, USA), a National Institutes of Health (NIH) Research Resource (Grant no. P41RR0954). Characterization of the nonmetallated peptide conjugates by ESI-MS was performed by SynBioSci (Livermore, CA, USA).

2.7. Radiolabeling of DTMA-(X)-BBN(7–14)NH_2 conjugates with $[^{99m}Tc(H_2O)_3(CO)_3]^+$

$Na[^{99m}TcO_4]$ was eluted from a $^{99m}Tc/^{99}Mo$ generator (Mallinckrodt Medical, St. Louis, MO, USA) using 0.9% saline. The $[^{99m}Tc(H_2O)_3(CO)_3]^+$ precursor was synthesized by adding $^{99m}TcO_4^-$ generator eluent (1 ml) to an Isolink kit (Tyco Healthcare, St. Louis, MO, USA), heating for 30 min in a water bath and then adding 0.1 M HCl (120μL). The $[^{99m}Tc(H_2O)_3(CO)_3]^+$ (500 μL) was added to a test tube containing purified peptide conjugate (100 μg, 74.3–86.7 nmol) and heated at 80°C for 1 h. Radiolabeled conjugates were purified by RP-HPLC and were collected into 100 μL of 1 mg/ml bovine serum albumin (BSA) stabilizing agent prior to in vitro and in vivo evaluation.

2.8. Stability of radiolabeled DTMA-(X)-BBN(7–14)NH^2 conjugates

The stability of radiometallated peptide conjugates was assessed in phosphate-buffered saline after 0, 1, 4 and 24 h incubation periods at room temperature (RT). RP-HPLC was used to asses the stability for each of the metallated conjugates. To assess the stability of the new conjugates to transmetallation reactions, histidine challenge experiments were performed. Briefly, each of the conjugates were incubated in 10^{-3} M histidine solution and analyzed by RP-HPLC. Assessment of stability was determined at 24 h post incubation with histidine solution.

2.9. In vitro competitive displacement binding assays of nonmetallated DTMA-(X)-BBN(7–14) NH_2 conjugates

The IC_{50} of DTMA-(X)-BBN(7–14)NH_2 was established by competitive displacement cell binding assays using radiolabeled ^{125}I-[Tyr^4]-BBN as the radioligand. Briefly, 3×10^4 cells (in D-MEM (Dulbecco's Modification of Eagle's Medium)/F-12K media containing 0.01 M MEM (minimum essential medium) and 2% BSA, pH=5.5) were incubated with 20,000 counts per minute ^{125}I-[Tyr^4]-BBN [8.2×10^{-15} mol, 8.14×10^4 GBq/mmol (2.20×10^3 Ci/mmol)] for 1 h at 37°C. Nonradiolabeled peptide conjugate was added at a steadily increasing concentration and allowed to incubate for an additional minute at 37°C. The solution was aspirated, and the cells were rinsed with cold media. Cell-associated radioactivity was determined using a Packard Riastar gamma counter.

2.10. In vitro internalization and externalization studies for $[^{99m}Tc(CO)_3$-DTMA-(X)-BBN(7–14) $NH_2]^+$ conjugates

The internalization studies were conducted by incubating 3×10^4 cells (in D-MEM/F-12K media containing 0.01 M MEM and 2% BSA, pH=5.5) in the presence of 20,000 counts per minute $[^{99m}Tc(CO)_3$-DTMA-(X)-BBN(7–14) $NH_2]^+$ (3.45×10^{-17} mol, 1.94×10^7 GBq/mmol (5.23×10^5 Ci/mmol) at 37°C. At 10, 20, 30, 45, 60, 90 and 120 min post incubation, the cells were aspirated, washed [0.2 N acetic acid/0.5 M NaCl (pH=2.5)] and counted on a Packard Riastar gamma counter. The externalization studies were completed after an initial 40 min internalization period. The cells were washed at RT, resuspended in media and incubated a second time. At 0, 20, 40, 60, 90, 120 and 150 min post incubation, the cells were washed with media and acetic acid/saline (pH=2.5 at 4°C) and counted on a Packard Riastar gamma counter.

2.11. Biodistribution studies of $[^{99m}Tc(CO)_3$-DTMA-(X)-BBN(7–14)$NH_2]^+$ conjugates

The pharmacokinetics of the $[^{99m}Tc(CO)_3$-DTMA-(X)-BBN(7–14)$NH_2]^+$ conjugates were determined in normal CF-1 and tumor-bearing PC-3 mouse models (*n*=5). All animal studies were conducted in accordance with the highest standards of care as outlined in the NIH guide for Care and Use of Laboratory Animals and the Policy and Procedures for Animal Research at the Harry S. Truman Memorial Veterans' Hospital. SCID mice bearing xenografted human PC-3 tumors were used to determine the ability to target tumor tissue in vivo. For studies involving tumor-bearing mice, 4–5-week old female ICR SCID outbred mice were obtained from Taconic (Germantown, NY, USA). The mice were housed five animals per cage in sterile microisolator cages in a temperature- and humidity-controlled room with a 12 h light/12 h dark schedule. The animals were fed autoclaved rodent chow (Ralston Purina, St. Louis, MO, USA) and water ad libitum. Animals were anesthetized for injections with isoflurane (Baxter Healthcare, Deerfield, IL, USA) at a rate of 2.5% with 0.4 L oxygen through a nonrebreathing anesthesia vaporizer. Human prostate PC-3 cells were injected on the bilateral subcutaneous flank with 5×10^6 cells in a suspension of 100 μl normal sterile saline per injection site. PC-3 cells were allowed to grow two to three weeks post inoculation, developing tumors ranging in mass from 0.02–1.30 g. Briefly, the mice were injected via the tail vein with 185 kBq (5 μCi) of conjugate in 100 μL of isotonic saline. Mice were euthanized at specific timepoints. Tissues, organs and urine were excised, weighed and counted in a NaI well counter. The percent injected dose (% ID) and the % ID per gram (% ID/g) were calculated. The whole blood volume was assumed to be 6.5% of the total body weight, allowing for the % ID in whole blood.

3. Results

DTMA was synthesized in a three-step procedure according to Scheme 1. Briefly, BOC protection of the primary amines of diethylenetriamine, alkylation of the secondary amine and subsequent ester hydrolysis afforded the product in good yield. The final product and product reaction intermediates were purified and fully characterized by ^1H and ^{13}C NMR and HR-FAB MS. DTMA was stored in a vial under nitrogen atmosphere. No decomposition was observed over a period of several months. DTMA peptide conjugates (Fig. 1) were synthesized by SPPS, purified by RP-HPLC and characterized by ESI-MS (Table 1). Radiolabeled conjugates were synthesized in a two-step procedure, according to Scheme 2. Radiolabeling yields were optimized by adjusting the pH of the solution containing the peptide conjugate and tricarbonyl precursor. Radiolabeled conjugates were afforded in ~90% yield. Single radiolabeled products were isolated by RP-HPLC (Fig. 2) and were stable over 24 h. Radiolabeled conjugates were also stable to 10^{-3} M histidine solution for periods ≤24 h.

Nonradioactive, metallated $[Re(CO)_3$-DTMA-(X)-BBN (7–14)$NH_2]^+$ conjugates were prepared in order to identify structurally (via ESI-MS) the macroscopic product in comparison to the tracer level $[^{99m}Tc(CO)_3$-DTMA-(X)-BBN(7–14)$NH_2]^+$ conjugates. Briefly, [Re $(CO)_3$-DTMA-(X)-BBN(7–14)$NH_2]^+$ conjugates were prepared by addition of an aqueous solution of $[Re(Br)_3(CO)_3]^{2-}$ to the DTMA (X)-BBN(7–14)NH_2 peptides with heating. These conjugates were purified by RP-HPLC and solvent removal in vacuo afforded the new conjugates as pale white solids. All of the calculated molecular ions for the Re(I) products matched experimental data (Table 1).

IC_{50} values for DTMA-(X)-BBN(7–14)NH_2 conjugates in human prostate PC-3 tumor cells using ^{125}I-[Tyr^4]-BBN as the radioligand are shown in Fig. 3. Single nanomolar IC_{50} values were obtained for all of the nonmetallated conjugates [GGG (2.58±1.3 nmol), GSG (0.65±0.3 nmol), SSS (0.77±0.2 nmol), β-Ala (0.29±0.2 nmol)], demonstrating the high affinity of these BBN(7–14)NH_2conjugates for the GRPr.

Internalization and externalization of [^{99m}Tc(CO)$_3$-DTMA-(X)-BBN(7–14)NH$_2$]$^+$ conjugates in human prostate PC-3 tumor cells is shown in Fig. 4 and Fig 5. The [^{99m}Tc(CO)$_3$-DTMA-(β-Ala)-BBN(7–14)NH$_2$]$^+$ conjugate exhibited rapid internalization with 18.7±0.03% internalized in 3×10^4 cells at 45 min. Internalization of conjugate increased slightly to 23.8 ±0.03% at 120 min post incubation. The [^{99m}Tc(CO)$_3$-DTMA-(X)-BBN(7–14)NH$_2$]$^+$ conjugates, where X=GGG, GSG and SSS, did not internalize at the same rate as [^{99m}Tc (CO)$_3$-DTMA-(β-Ala)-BBN(7–14)NH$_2$]$^+$, with only 2.37±0.01%, 6.59±0.04% and 11.46 ±0.03% internalizing at 120 min, respectively. [^{99m}Tc(CO)$_3$-DTMA-(β-Ala)-BBN(7–14) NH$_2$]$^+$ conjugate also exhibited favorable externalization properties from PC-3 cells, where after 90-min incubation in media, 90.1±0.12% remained internalized in the cells. [^{99m}Tc (CO)$_3$-DTMA-(X)-BBN(7–14)NH$_2$]$^+$ conjugates, where X=GGG, GSG and SSS, externalized more rapidly than [^{99m}Tc(CO)$_3$-DTMA-(β-Ala)-BBN(7–14)NH$_2$]$^+$, with only 57.0±0.17%, 51.3±0.09% and 74.7±0.11% of administered tracer remaining in PC-3 cells at the end of the 90-min incubation period.

Table 2 summarizes the results of biodistribution studies for [^{99m}Tc(CO)$_3$-DTMA-(X)-BBN (7–14)NH$_2$]$^+$ conjugates in CF-1 normal mice. The mice were sacrificed at 1 h post injection (p.i.), and tissues and organs were excised and counted in a NaI well counter. Rapid clearance from blood was observed for all of the conjugates at 1 h p.i., with the exception of the conjugate where X=SSS, with a blood retention of 2.73±0.40% ID/g. Excretion of the conjugates varied. The more hydrophilic serine-containing pharmacokinetic modifiers emptied primarily via the renal-urinary excretion system. On the other hand, the hydrophobic conjugates, where X=β-Ala and GGG, were excreted primarily via the hepatobiliary system. High affinity of conjugates to GRP receptor-expressing pancreas was shown in this study. The pancreas uptake in normal mice was 19.42±4.31% ID/g for X=β-Ala, 10.36±0.90% ID/g for X=GGG, 15.48±5.25% ID/g for X=GSG and 8.00±0.88% ID/g for X=SSS. Blocking studies, in which high levels of cold BBN(1–14) was administered 15 min prior to the [^{99m}Tc(CO)$_3$-DTMA-(X)-BBN(7–14) NH$_2$]$^+$ conjugate, reduced the % ID/g uptake/retention in normal pancreas by a factor of 8–10. This clearly identifies the affinity of these conjugates for the GRPr. Table 3 summarizes the results of biodistribution studies for the [^{99m}Tc(CO)$_3$-DTMA-(β-Ala)-BBN(7–14)NH$_2$]$^+$ conjugate in SCID mice bearing xenografted, human, PC-3 tumors at 1, 4 and 24 h p.i. The conjugate's rate of clearance from whole blood was very rapid, with only 0.73±0.60% ID/g at 1 h p.i., 0.37±.24% ID/g at 4 h p.i. and 0.11±0.04% ID/g at 24 h p.i. remaining in tissue. The average tumor uptake for the [^{99m}Tc(CO)$_3$-DTMA-(β-Ala)-BBN(7–14)NH$_2$]$^+$ conjugate was 0.95±0.15% ID/g at 1 h p.i., 0.52±0.10% ID/g at 4 h p.i. and 0.13±0.07% ID/g at 24 h p.i. Receptor-mediated pancreatic uptake was 8.20±2.38% ID/g at 1 h p.i., 8.27±2.47% ID/g at 4 h p.i. and 4.12±1.23% ID/g at 24 h p.i.

4. Discussion

Small peptides continue to be effective delivery vehicles for diagnostic and therapeutic radionuclides due to their ability to bind receptors expressed on specific human cancers [26, 27]. The model of success in this arena has been Octreoscan ([^{111}In-DTPA-Octreotide]), with its targeting and diagnostic imaging of somatostatin receptor-positive neuroendocrine tumors [28]. As a result of this success, there is a basis for investigating in diagnostic and therapeutic radiopharmaceuticals based upon other peptides, including BBN, alpha-melanocyte stimulating hormone, vasoactive intestinal peptide, cholecystokinin and neurotensin [27,29].

In the past decade, our group and many others have been interested in designing and developing radiotracers that target the BBN receptor superfamily [3–9,30]. Radiolabeled targeting vectors based upon BBN have proven to be highly selective for BBN receptors, including the GRPr [31]. Diagnostic and therapeutic radiopharmaceuticals based upon BBN hold some promise for molecular imaging and treatment of GRP receptor-expressing tumors of the breast and

prostate [3,7,27,31]. In this study, we have developed [^{99m}Tc(CO)$_3$-DTMA-(X)-BBN(7–14)NH$_2$]$^+$ conjugates and studied the influence of the pharmacokinetic modifier, X, on the binding affinity, internalization, externalization and biodistribution properties for this series of radiopharmaceuticals.

Moderately soft amine donor atoms have been widely used in coordinating ^{99m}Tc to produce kinetically inert complexes for in vivo diagnostic imaging procedures [32,33]. Studies of *fac*-[^{99m}Tc(CO)$_3$]$^+$ metal centers bound to aromatic *N*-heterocycles and coordinating carboxylic acids have exhibited ideal in vivo stability and clearance characteristics, demonstrating the need for further radiopharmaceutical development [18]. Our group, however, has demonstrated the efficacy of using bidentate aliphatic primary amines to coordinate the *fac*-[^{99m}Tc(CO)$_3$]$^+$ metal center, resulting in kinetically inert conjugates of BBN. These conjugates produced high quality microSPECT images in mice bearing xenografted PC-3 tumors [25,34,35]. Our group has also investigated tridentate ligand frameworks, which include the DTMA. A tridentate ligand framework is able to coordinate the *fac*-[^{99m}Tc(CO)$_3$]$^+$ metal fragment at three sites on the metal center. This all but eliminates destabilization of the metal center by transmetalation reactions in the presence of serum proteins. In this study, the DTMA ligand was synthesized by conventional methods and conjugated to the N-terminal primary amine of H$_2$N-(X)-BBN(7–14)NH$_2$. DTMA-(X)-BBN(7–14)NH$_2$ conjugates were produced and displayed good selectivity and affinity for the GRPr. Competitive displacement of ^{125}I-[Tyr^4]-BBN from human prostate PC-3 cells by DTMA-(X)-BBN(7–14) NH$_2$ showed that the DTMA-(X)-BBN(7–14)NH$_2$ conjugates had very high affinity to the GRPr expressed on this cell line. [^{99m}Tc(CO)$_3$-DTMA-(X)-BBN(7–14)NH$_2$]$^+$ conjugates were produced in high radiochemical yield using the Isolink [^{99m}Tc(H$_2$O)$_3$(CO)$_3$]$^+$ kit. Their affinity for the GRPr was tested in vitro and in vivo. Attempts to radiolabel H$_2$N-(β-Ala)-BBN(7–14)NH$_2$ were unsuccessful, providing solid evidence for coordination of the *fac*-[^{99m}Tc(CO)$_3$]$^+$ metal center to the tridentate ligand's two primary amines and tertiary amine. The tridentate DTMA ligand provided effective containment of the *fac*-[^{99m}Tc(CO)$_3$]$^+$ metal center, with metallated conjugates being stable in 10^{-3} M histidine solution for periods exceeding 20 h.

High-quality, high-contrast SPECT images require maximum uptake and residualization of radiotracer in receptor-expressing cells. Internalization and externalization studies showed some degree of variation in uptake and retention of radioactivity in viable cells. [^{99m}Tc(CO)$_3$-DTMA-(β-Ala)-BBN(7–14)NH$_2$]$^+$ showed the highest uptake and very slow externalization from PC-3 cells. This is presumably due to the inability of lysosomal proteases to fragment the aliphatic β-Ala linker as compared to the amino acid linkers. Cell-surface receptor binding of these agonistic ligands promotes receptor-mediated endocytosis, which results in optimum accumulation and retention of radioactivity within the cell. For all of the conjugates in this study, cell-associated radioactivity was found to be internalized and not surface bound.

Rodent pancreas has been shown to express the GRPr in very high numbers [36–39]. Therefore, accumulation of radioactivity in normal rodent model pancreas can be used as a means of quality control to ascertain the degree of effective GRPr targeting for the [^{99m}Tc(CO)$_3$-DTMA-(X)-BBN(7–14) NH$_2$]$^+$ conjugates in vivo. Biodistribution studies for the [^{99m}Tc(CO)$_3$-DTMA-(X)-BBN(7–14)NH$_2$]$^+$ conjugates in CF-1 normal mice showed receptor-mediated accumulation of radioactivity in normal pancreas ranging from 8–20% ID/g. [^{99m}Tc(CO)$_3$-DTMA-(β-Ala)-BBN(7–14)NH$_2$]$^+$ showed the highest degree of receptor-mediated pancreatic accumulation at 1 h p.i. and favorable in vitro internalization in PC-3 cells. Therefore, this conjugate was selected for further studies in PC-3 tumor-bearing SCID mouse model. Experimental results for [^{99m}Tc(CO)$_3$-DTMA-(β-Ala)-BBN (7–14)NH$_2$]$^+$ in PC-3 tumor-bearing mice were not nearly as favorable as was expected. Average tumor uptake for the [^{99m}Tc(CO)$_3$-DTMA-(β-Ala)-BBN(7–14)NH$_2$]$^+$ conjugate was 0.95±0.15% ID/g at 1 h p.i.

This value is comparable to other tridentate ^{99m}Tc-conjugates reported in the literature [11, 30,36,40]. La Bella et al. [41] have demonstrated the utility of [^{99m}Tc(CO)$_3$-PADA-AVA]BBN(7–14) (where PADA=2-picolylamine-*N*,*N*′-diacetic acid and AVA=5-aminovaleric acid) to target the GRPr in normal pancreas (8.45±0.93% ID/g at 1.5 h p.i.) of PC-3 tumor-bearing CD-1 mice. However, uptake in tumor was only 0.59±0.11% ID/g at 1.5 h p.i. [41]. Labella et al. have also reported on [^{99m}Tc (CO)$_3$-N_α-histidinyl acetate]BBN(7–14), in which receptor-mediated uptake of the conjugate in nu/nu CD-1 mice bearing PC-3 tumors was only 0.32±0.10% ID/g at 1.5 h p.i. [30]. In each of these two cases, low accumulation of radioactivity in tissue was presumably due to poor vascularization of the tumor [30,41]. It was not possible to directly compare differences in tumor accumulation between [^{99m}Tc(CO)$_3$-PADA-AVA]BBN(7–14), [^{99m}Tc(CO)$_3$-N_α-histidinyl acetate]BBN(7–14) and [^{99m}Tc(CO)$_3$-DTMA-(β-Ala)-BBN(7–14)NH$_2$]$^+$ due to minor structural modifications between conjugates and differences in the animal model. However, in the case of [^{99m}Tc(CO)$_3$-DTMA-(β-Ala)-BBN(7–14)NH$_2$]$^+$, reduced accumulation of conjugate in PC-3 tumors is not likely to be due to poor tumor vascularization. Under physiological conditions, carbon-nitrogen cleavage of the pendant aliphatic arm of the tertiary amine nitrogen could result in metabolized reaction byproducts and lower accumulation in tumor tissue. However, this too was unlikely since the molecular cleavage reaction mechanism occurs most often during formation of the tertiary amine complex [42]. Fully coordinated conjugates are not generally susceptible to C–N bond cleavage [42]. Reduced accumulation of the [^{99m}Tc(CO)$_3$-DTMA-(β-Ala)-BBN(7–14)NH$_2$]$^+$ conjugate in tumor was presumably due to the lipophilic nature of the radiotracer and rapid hepatobiliary uptake and excretion on first pass extraction of the radiopharmaceutical.

5. Conclusion

DTMA provided a versatile synthetic route via traditional SPPS to produce new peptide conjugates that were easily radiolabeled with the *fac*-[^{99m}Tc(CO)$_3$]$^+$ metal center using the Isolink radiolabeling kit. DTMA-(X)-BBN(7–14)NH$_2$ formed well-defined conjugates in good yield upon radiolabeling with the [^{99m}Tc(H$_2$O)$_3$(CO)$_3$]$^+$ precursor. [^{99m}Tc (CO)$_3$-DTMA-(X)-BBN(7–14)NH$_2$]$^+$ conjugates presented some variability in excretion properties depending upon the pharmacokinetic modifier that was chosen. All of the conjugates displayed very high affinity and selectivity for the GRPr in vitro and in vivo. [^{99m}Tc(CO)$_3$-DTMA-(β-Ala)-BBN(7–14)NH$_2$]$^+$ showed the highest degree of receptor-mediated pancreatic accumulation in normal CF-1 mice and very favorable internalization and externalization properties in PC-3 cells in vitro. Studies in the PC-3 tumor-bearing SCID mouse model, however, showed relatively low accumulation in tumor tissue, presumably due to rapid first-pass accumulation into the hepatobiliary system. Studies are currently underway to evaluate and optimize new [^{99m}Tc(CO)$_3$-DTMA-(X)-BBN(7–14)NH$_2$]$^+$ conjugates having very high affinity for GRP receptor-expressing tumors for in vivo molecular imaging via SPECT.

Acknowledgments

This material was the result of work supported with resources and the use of facilities at the Harry S. Truman Memorial Veterans' Hospital. Columbia, MO, 65201 and the University of Missouri-Columbia School of Medicine, Columbia, MO 65211, USA. This work was funded in part by The United States Department of Veterans' Affairs VA Merit Award. Salary support for T.L.R. and G.L.S. also acknowledges the National Institutes of Health (1 P50 CA103130-01).

References

1. West SD, Mercer DW. Bombesin-induced gastroprotection. Ann Surg 2005;241:227–231. [PubMed: 15650631]
2. Fleischmann A, Läderach U, Friess H, Buechler MW, Reubi JC. Bombesin receptors in distinct tissue compartments of human pancreatic diseases. Lab Invest 2000;80:1807–1817. [PubMed: 11140694]

3. Prasanphanich AF, Nanda PK, Rold TL, Ma L, Lewis MR, Garrison JC, et al. [^{64}Cu-NOTA-8-Aoc-BBN(7–14)NH_2] Conjugate: a novel targeting vector for positron emission tomographic imaging of gastrin releasing peptide receptor-expressing tissues. Proc Natl Acad Sci U S A 2007;104:12462–12467. [PubMed: 17626788]
4. Garrison JC, Rold TL, Sieckman GL, Figueroa SD, Volkert WA, Jurisson SS, et al. In vivo evaluation and small-animal PET/CT of a prostate cancer mouse model using ^{64}Cu bombesin analogs: side-by-side comparison of the CB-TE2A and DOTA chelation systems. J Nucl Med 2007;48:1327–1337. [PubMed: 17631556]
5. de Visser M, Bernard HF, Erion LJ, Schmidt MA, Srinivasan A, Waser B, et al. Novel ^{111}In-labelled bombesin analogues for molecular imaging of prostate tumors. Eur J Nucl Med Mol Imaging 2007;34:1228–1238. [PubMed: 17287960]
6. Biddlecombe GB, Rogers BE, de Visser M, Parry JJ, de Jong M, Erion JL, et al. Molecular imaging of gastrin-releasing peptide receptor-positive tumors in mice using ^{64}Cu- and ^{86}Y-DOTA-(Pro^1,Tyr^4)-bombesin(1–14). Bioconjug Chem 2007;18:724–730. [PubMed: 17378600]
7. Parry JJ, Andrews R, Rogers BE. MicroPET imaging of breast cancer using radiolabeled bombesin analogs targeting the gastrin-releasing peptide receptor. Breast Cancer Res Treat 2007;101:175–183. [PubMed: 16838112]
8. Lantry LE, Cappelletti E, Maddalena ME, Fox JS, Feng F, Chen J, et al. ^{177}Lu-AMBA: synthesis and characterization of a selective ^{177}Lu-labeled GRP-R agonist for systemic radiotherapy of prostate cancer. J Nucl Med 2006;47:1144–1152. [PubMed: 16818949]
9. Zhang X, Cai W, Cao F, Schreibmann E, Wu Y, Wu JC, et al. ^{18}F-labeled bombesin analogs for targeting GRP receptor-expressing prostate cancer. J Nucl Med 2006;47:492–501. [PubMed: 16513619]
10. Montet X, Yuan H, Weissleder R, Josephson L. Enzyme-based visualization of receptor-ligand binding in tissues. Lab Invest 2006;86:517–525. [PubMed: 16568109]
11. Garcia-Garayoa E, Ruegg D, Blauenstein P, Zwimpfer M, Khan IU, Maes V, et al. Chemical and biological characterization of new Re $(CO)_3$/[^{99m}Tc]$(CO)_3$ bombesin analogues. Nucl Med Biol 2007;34:17–28. [PubMed: 17210458]
12. Parry JJ, Kelly TS, Andrews R, Rogers BE. In vitro and in vivo evaluation of ^{64}Cu-labeled DOTA-linker-bombesin(7–14) analogues containing different amino acid linker moieties. Bioconjug Chem 2007;18:1110–1117. [PubMed: 17503761]
13. Veerendra B, Sieckman GL, Hoffman TJ, Rold T, Retzloff L, McCrate J, et al. Synthesis, radiolabeling and in vitro GRP receptor targeting studies of ^{99m}Tc-Triaza-X-BBN[7–14]NH_2 (*X*=serylserylserine, glycylglycylglycine, glycylserylglycine, or beta-alanine). Synth React Inorg Met-Org Nano-Met Chem 2006;36:481–491.
14. Marti N, Spingler B, Schibli R. Comparative studies of substitution reactions of rhenium(I) dicarbonyl-nitrosyl and tricarbonyl complexes in aqueous media. Inorg Chem 2005;44:6082–6091. [PubMed: 16097829]
15. Méndez-Rojas MA, Kharisov BI, Tsivadze AY. Recent advances on technetium complexes: coordination chemistry and medical applications. J Coord Chem 2006;59:1–63.
16. Banerjee SR, Babich JW, Zubieta J. A new bifunctional amino acid chelator targeting the glucose transporter. Inorganica Chim Acta 2006;359:1603–1612.
17. Schibli R, Schubiger PA. Current use and future potential of organo-metallic radiopharmaceuticals. Eur J Nucl Med 2002;29:1529–1542.
18. Abram U, Alberto R. Technetium and rhenium—coordination chemistry and nuclear medical applications. J Braz Chem Soc 2006;17:1486–1500.
19. Maria L, Cunha S, Videira M, Gano L, Paulo A, Santos IC. Rhenium and technetium tricarbonyl complexes anchored by pyrazole-based tripods: novel lead structures for the design of myocardial imaging agents. Dalton Trans 2007;28:3010–3019. [PubMed: 17622418]
20. Banerjee SR, Babich JW, Zubieta J. Bifunctional chelates with aliphatic amine donors for labeling of biomolecules with the $\{Tc(CO)_3\}^+$ and $\{Re(CO)_3\}^+$ cores: the crystal and molecular structure of $[Re(CO)_3\{(H_2NCH_2CH_2)_2N(CH_2)_4CO_2Me\}]Br$. Inorg Chem Commun 2004;7:481–484.

21. Wei L, Babich J, Zubieta J. Bifunctional chelates with mixed aromatic and aliphatic amine donors for labeling of biomolecules with the $\{Tc(CO)_3\}^+$ and $\{Re(CO)_3\}^+$ cores. Inorganica Chim Acta 2005;358:3691–3700.
22. Pearson RG. Hard and soft acids and bases. J Am Chem Soc 1963;85:3533–3539.
23. Pearson RG. Hard and soft acids and bases, part I, fundamental principles. J Chem Ed 1968;45:581–587.
24. Pearson RG. Hard and soft acids and bases, part II, underlying theories. J Chem Ed 1968;45:643–648.
25. Prasanphanich AF, Lane SR, Figueroa SD, Ma L, Rold TL, Sieckman GL, et al. The effects of linking substituents on the in vivo behavior of site-directed, peptide-based. In vivo 2007;21:1–16. [PubMed: 17354608]
26. Rogers BE, Bigott HM, McCarthy DW, Manna DD, Joonyoung K, Sharp TL, et al. MicroPET imaging of a gastrin-releasing peptide receptor-positive tumor in a mouse model of human prostate cancer using a 64Cu-labeled bombesin analogue. Bioconjugate Chem 2003;14(4):756–763.
27. van der Lely AJ, de Herder WW, Krenning EP, Kwekkeboom DJ. Octreoscan radioreceptor imaging. Endocrine 2003;20:307–311. [PubMed: 12721512]
28. Garcia-Garayoa E, Maes V, Blaeuenstein P, Blanc A, Hohn A, Tourwe D, et al. Double-stabilized neurotensin analogues as potential radiopharmaceuticals for NTR-positive tumors. Nucl Med Bio 2006;33:495–503. [PubMed: 16720241]
29. Okarvi SM. Peptide-based radiopharmaceuticals: future tools for diagnostic imaging of cancers and other diseases. Med Res Rev 2004;24:357–397. [PubMed: 14994368]
30. Smith CJ, Volkert WA, Hoffman TJ. Radiolabeled peptide conjugates for targeting of the bombesin receptor superfamily subtypes. Nucl Med Bio 2005;32:733–740. [PubMed: 16243649]
31. Bandoli G, Tisato F, Dolmella A, Agostini S. Structural overview of technetium compounds (2000–2004). Coord Chem Rev 2006;250:561–573.
32. Jurisson SS, Lydon JD. Potential technetium small molecule radiopharmaceuticals. Chem Rev 1999;99:2205–2218. [PubMed: 11749479]
33. Smith CJ, Sieckman GL, Owen NK, Hayes DL, Mazuru DG, Volkert WA, et al. Radiochemical investigations of [$^{188}Re(H_2O)(CO)_3$-diaminopropionic acid-SSS-bombesin(7–14)NH_2]: syntheses, radiolabeling and in vitro/in vivo GRP receptor targeting studies. Anticancer Res 2003;23:63–70. [PubMed: 12680195]
34. Smith CJ, Sieckman GL, Owen NK, Hayes DL, Mazuru DG, Kannan R, et al. Radiochemical investigations of gastrin-releasing peptide receptor-specific [$^{99m}Tc(X)(CO)_3$-Dpr-Ser-Ser-Ser-Gln-Trp-Ala-Val-Gly-His-Leu-Met-(NH_2)] in PC-3, tumor-bearing, rodent models: syntheses, radiolabeling, and in vitro/in vivo studies where Dpr=2,3-diaminopropionic acid and X=H_2O or P($CH_2OH)_3$. Cancer Res 2003;63:4082–4088. [PubMed: 12874010]
35. Varga G, Reidelberger RD, Liehr RM, Bussjaeger LJ, Coy DH, Solomon TE. Effects of potent bombesin antagonist on exocrine pancreatic secretion in rats. Peptides 1991;12:493–497. [PubMed: 1717952]
36. Fanger BO, Wade AC, Cardin AD. Characterization of the murine pancreatic receptor for gastrin releasing peptide and bombesin. Regul Pept 1991;32:241–251. [PubMed: 1650953]
37. Huang SC, Yu DH, Wank SA, Gardner JD, Jensen RT. Characterization of the bombesin receptor on mouse pancreatic acini by chemical cross-linking. Peptides 1990;11:1143–1150. [PubMed: 1708135]
38. Kane MA, Kelley K, Ross SE, Portanova LB. Isolation of a gastrin releasing peptide receptor from normal rat pancreas. Peptides 1991;12:207–213. [PubMed: 1648710]
39. La Bella R, Garcia-Garayoa E, Baehler M, Blaeuenstein P, Schibli R, Conrath P, et al. A $^{99m}Tc(I)$-postlabeled high affinity bombesin analogue as a potential tumor imaging agent. Bioconjugate Chem 2002;13:599–604.
40. Alves S, Correia JDG, Santos I, Veerendra B, Sieckman GL, Hoffman TJ, et al. Pyrazolyl conjugates of bombesin: a new tridentate ligand framework for the stabilization of fac-$[M(CO)_3]^+$ moiety. Nucl Med Biol 2006;33:625–634. [PubMed: 16843837]
41. La Bella R, Garcia-Garayoa E, Langer M, Bläuenstein P, Beck-Sickinger AG, Schubiger PA. In vitro and in vivo evaluation of a ^{99m}Tc (I)-labeled bombesin analogue for imaging of gastrin releasing peptide receptor-positive tumors. Nucl Med and Biol 2002;29:553–560. [PubMed: 12088725]

42. Mundwiler S, Candreia L, Häfliger P, Ortner K, Alberto R. Preparation of no-carrier-added technetium-99m complexes via metal-assisted cleavage from a solid phase. Bioconjugate Chem 2004;15:195–202.

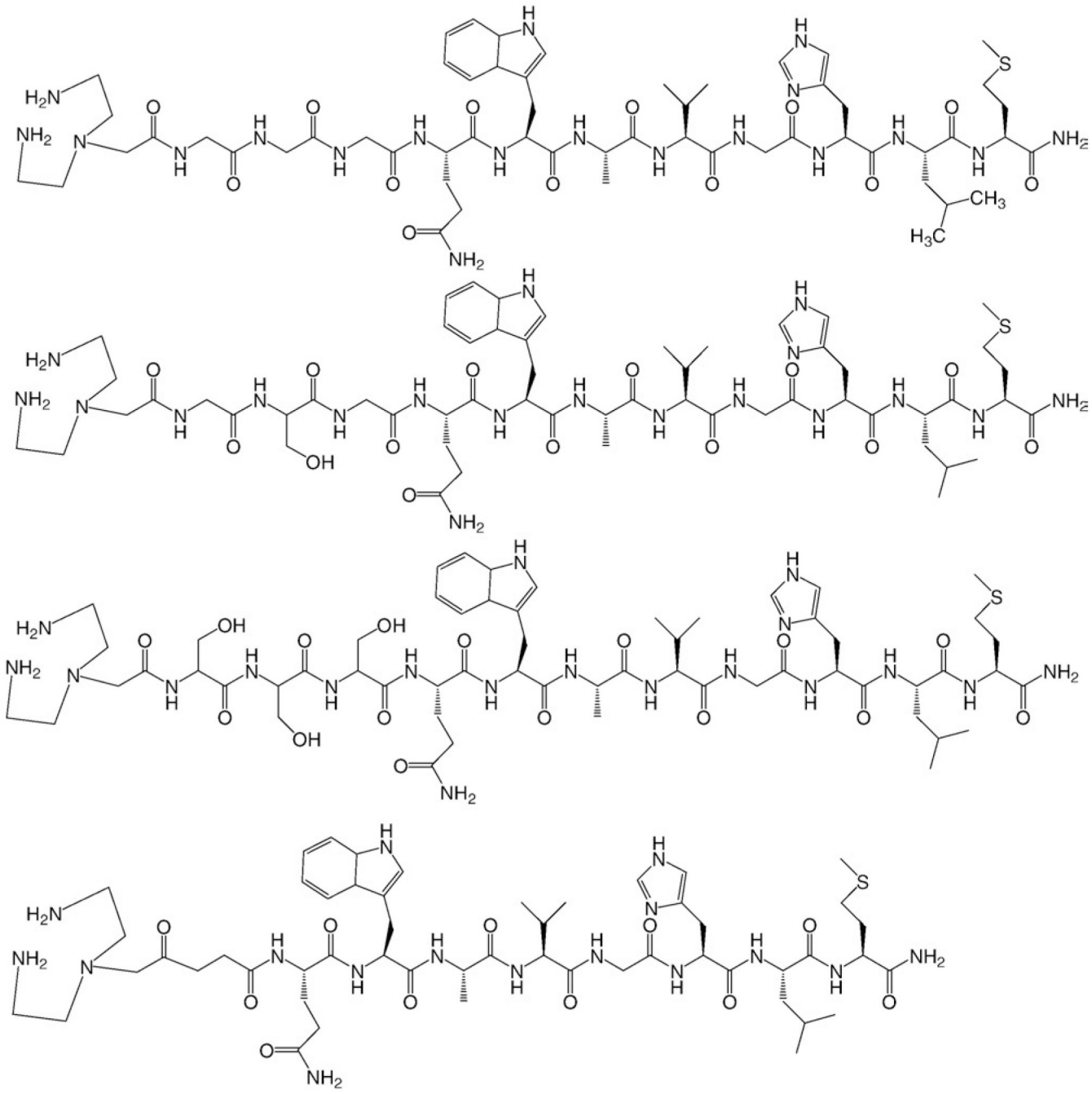

Fig. 1.
Structure of DTMA-(X)-BBN(7–14)NH_2, where X=GGG (top), GSG, SSS and β-Ala (bottom).

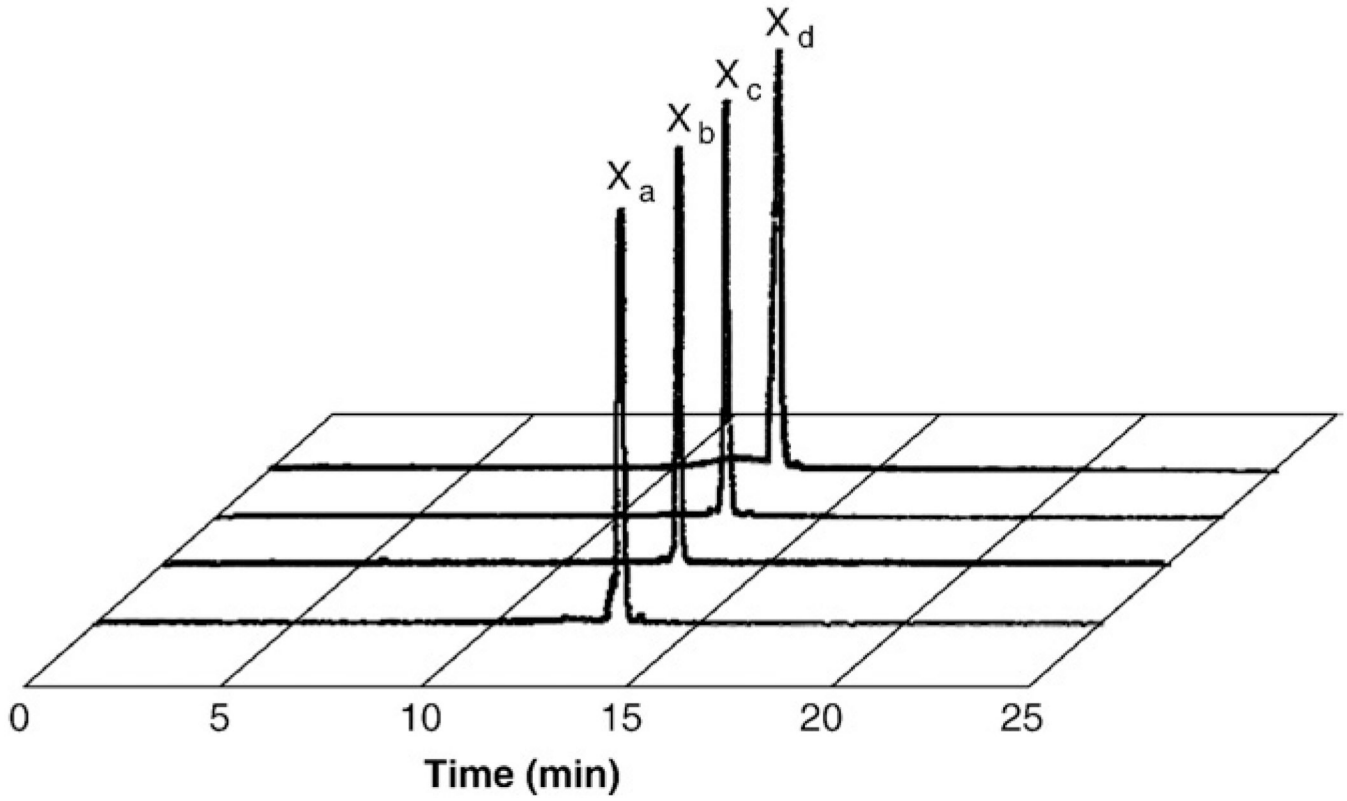

Fig. 2.

HPLC chromatographic profiles of $[^{99m}Tc(CO)_3$-DTMA-(X)-BBN(7–14)$NH_2]^+$ conjugates, where X_a=β-Ala (13.0 min), X_b=GGG (12.7 min), X_c=GSG (12.6 min) and X_d=SSS (12.5 min).

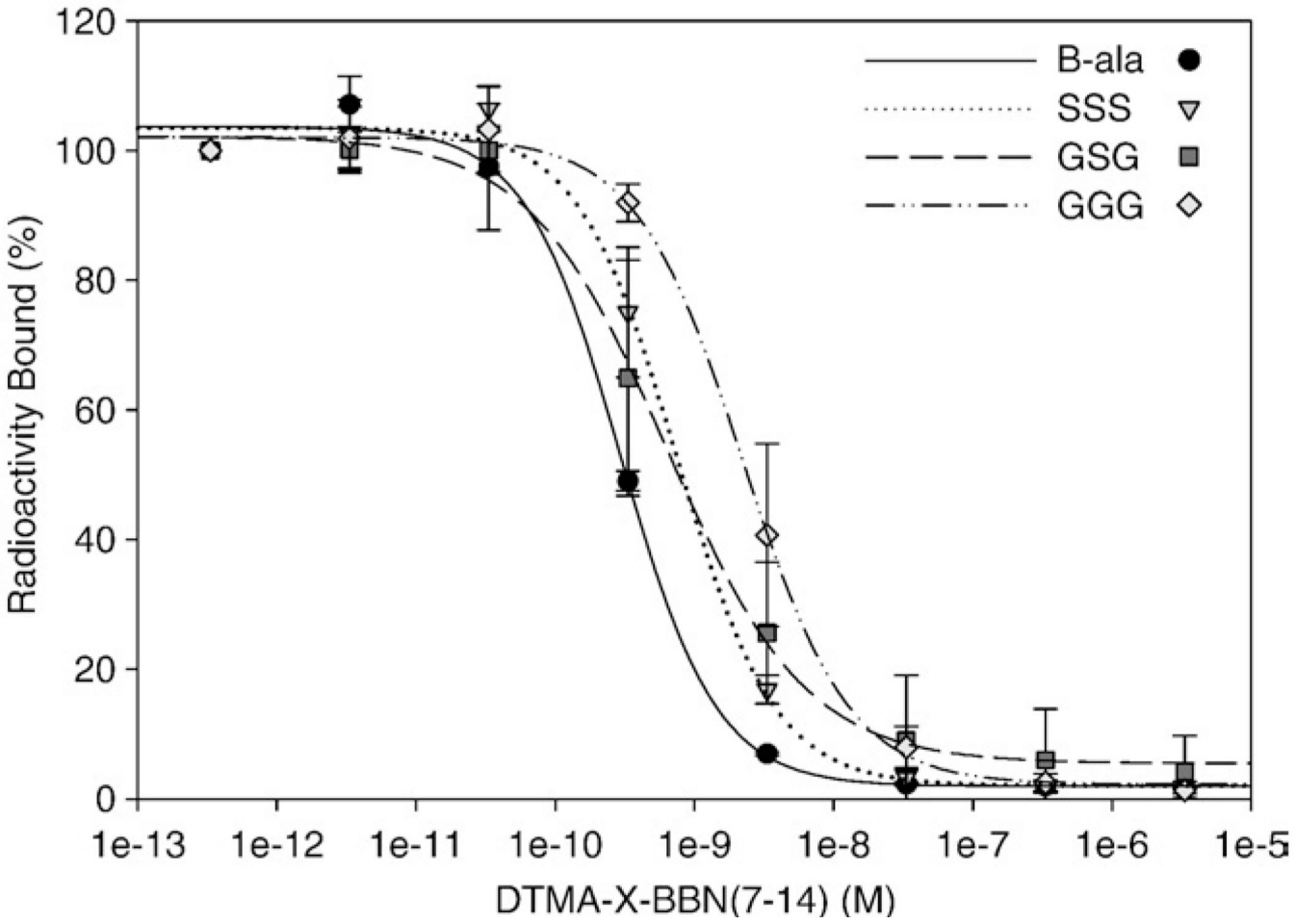

Fig. 3.

IC_{50} data of DTMA-(X)-BBN(7–14)NH_2 peptides versus bound [^{125}ITyr^4-BBN] conjugate, for X=β-Ala (0.28±0.2 nM), GGG (2.56±1.3 nM), GSG (0.68±0.3 nM) and SSS (0.74±0.2 nM).

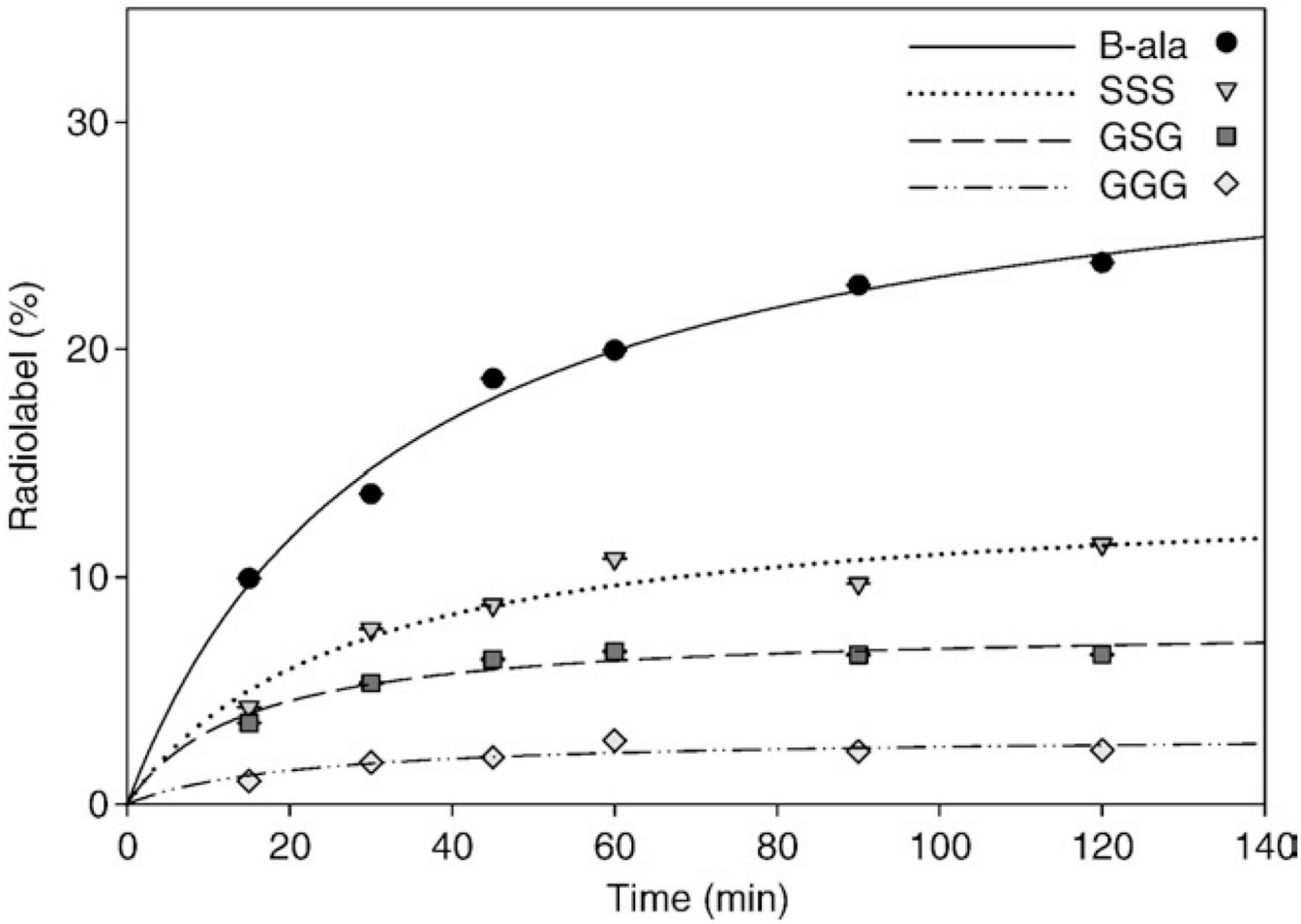

Fig. 4.

Internalization data, percentage of $[^{99m}Tc(CO)_3$-DTMA-(X)-BBN(7–14)$NH_2]^+$ conjugates cell-associated radioactivity internalized versus time, for X=β-Ala (solid line), GGG (dashed line), GSG (dotted line) and SSS (intermittently dashed line).

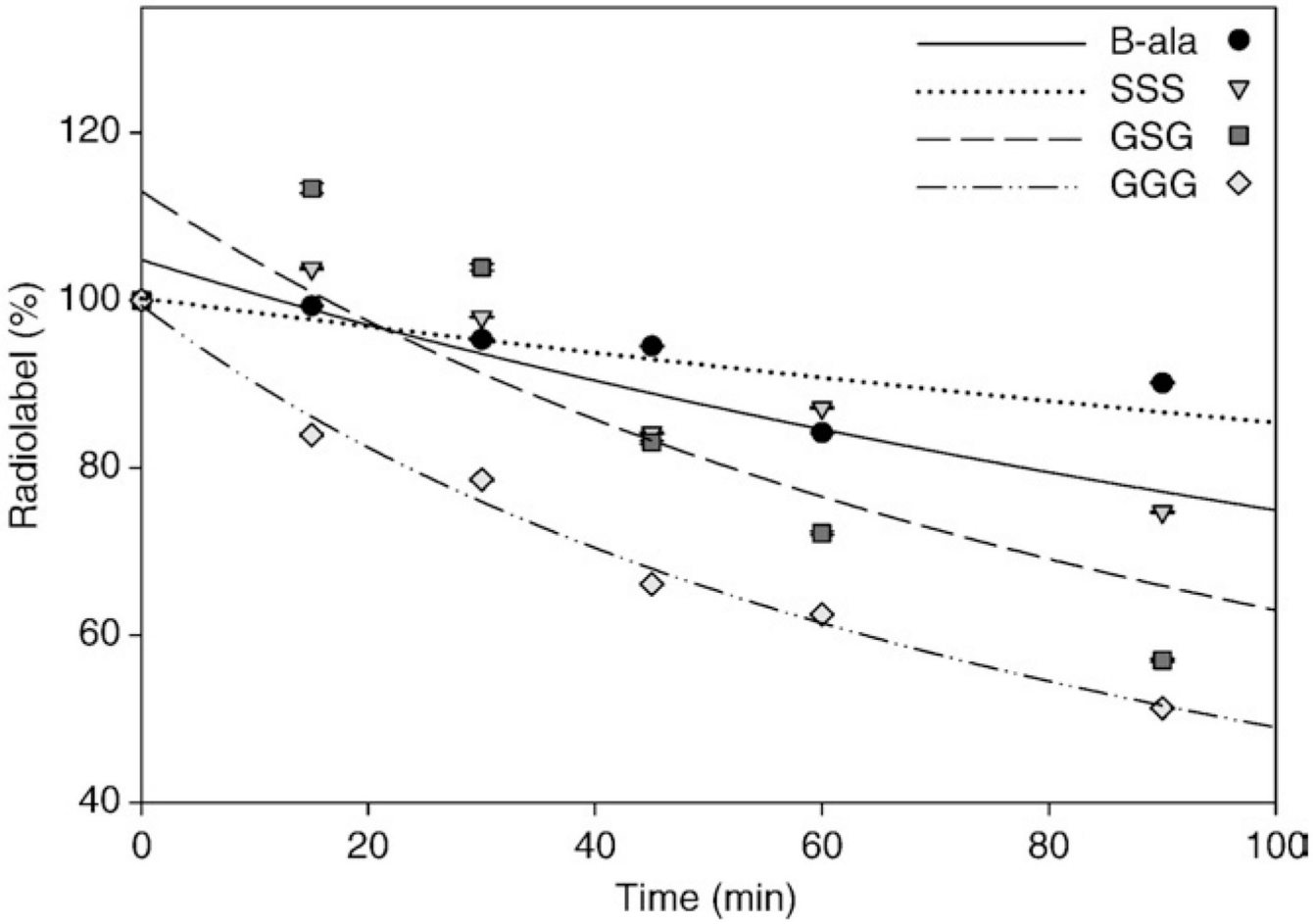

Fig. 5.

Externalization data, percentage of initial [^{99m}Tc(CO)$_3$-DTMA-(X)-BBN(7–14)NH$_2$]$^+$ conjugates remaining internalized versus time for X=β-Ala (solid line), GGG (dashed line), GSG (dotted line) and SSS (intermittently dashed line).

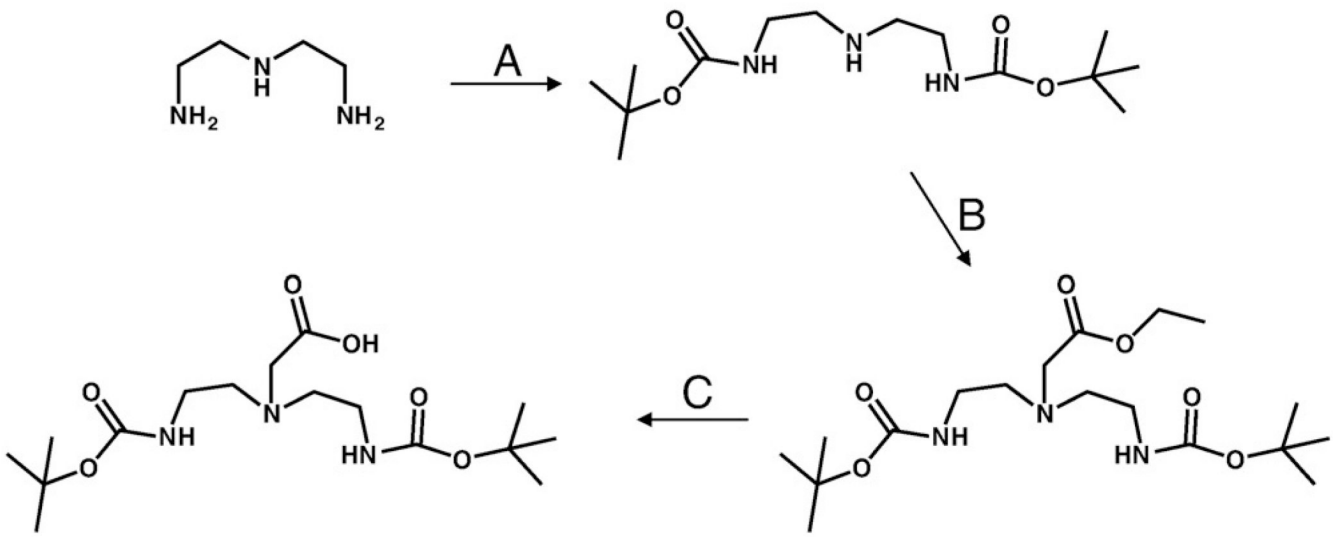

Scheme 1.

Synthesis of BOC-DTMA-acid. (A) BOC-ON, THF 0°C, 4 h; (B) $BrCH_2COOC_2H_5$, $N(Et)_3$, KI, CH_3CN, Δ, 6 h; (C) MeOH, 5% NaOH, RT, 3 h.

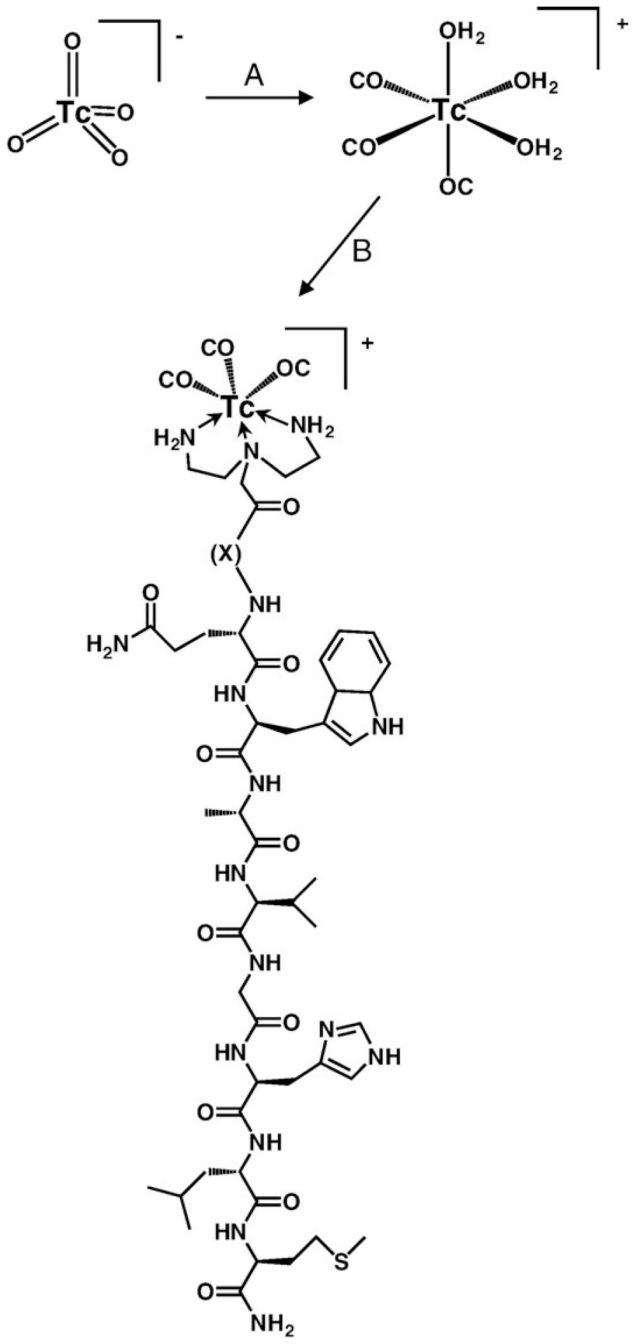

Scheme 2.
Radiolabeling scheme for [^{99m}Tc(CO)$_3$-DTMA-(X)-BBN(7–14) NH$_2$]$^+$ conjugates. (A) Isolink® kit, 120μL 0.1 HCl, 100°C, 25 min; (B) peptide conjugate 80°C, 1 h.

Table 1

Electrospray mass spectrometry values of DTMA-(X)-BBN(7–14)NH_2 and [$Re(CO)_3$-DTMA-(X)-BBN(7–14)NH_2]$^+$conjugates

DTMA-X-BBN(7–14)NH_2	Molecular formula	Calculated	Experimental
X=β-ala	$C_{52}H_{83}N_{17}O_{11}S$	1153.6	1152.7
	$C_{55}H_{83}N_{17}O_{14}SRe$	1424.6	1424.0
X=GGG	$C_{55}H_{89}N_{19}O_{13}S$	1255.6	1254.4
	$C_{58}H_{89}N_{19}O_{16}SRe$	1526.7	1525.2
X=GSG	$C_{56}H_{91}N_{19}O_{14}S$	1285.6	1284.9
	$C_{59}H_{91}N_{19}O_{17}SRe$	1556.8	1553.1
X=SSS	$C_{58}H_{95}N_{19}O_{16}S$	1346.5	1344.7
	$C_{61}H_{95}N_{19}O_{19}SRe$	1616.8	1616.8

Table 2

Biodistribution of $[^{99m}Tc(CO)_3$-DTMA-(X)-BBN(7–14)$NH_2]^+$ conjugates in CF-1 normal mice at 1 h p.i. (*n*=5, % ID/g±S.D.)

Tissue/organ	X=β-ala	X=GGG	X=GSG	X=SSS
Bladder	0.65 (0.38)	1.17 (0.81)	1.41 (1.58)	3.52 (2.77)
Heart	0.15 (0.04)	1.86 (029)	0.40 (0.21)	1.58 (0.15)
Lungs	0.26 (0.04)	0.46 (0.10)	0.49 (0.27)	2.55 (0.28)
Liver	7.48 (0.87)	9.52 (1.29)	5.49 (2.12)	6.38 (0.96)
Kidney	3.49 (0.65)	2.30 (0.50)	3.39 (2.0)	6.37 (0.30)
Spleen	1.16 (0.17)	0.47 (0.08)	1.09 (0.54)	0.97 (0.12)
Stomach	1.03 (0.50)	2.27 (1.23)	0.96 (0.42)	0.82 (0.26)
Small intestine	20.52 (2.73)	16.97 (2.93)	5.92 (1.85)	5.07 (0.79)
Large Intestine	3.37 (1.00)	9.14 (2.55)	4.07 (0.91)	1.81 (0.50)
Muscle	0.12 (0.06)	0.20 (0.07)	0.11 (0.07)	0.43 (0.06)
Bone	0.30 (0.16)	0.19 (0.04)	0.23 (0.08)	0.80 (0.22)
Brain	0.03 (0.01)	0.02 (0.01)	0.03 (0.02)	0.21 (0.15)
Pancreas	19.43 (4.31)	10.36 (0.90)	15.48 (5.25)	8.00 (0.88)
Blood	0.22 (0.02)	0.17 (0.04)	0.32 (0.13)	2.73 (0.40)
Urine	41.37 (2.77)	38.31 (23.68)	63.75 (13.03)	57.69 (4.04)

Table 3

Biodistribution of $[^{99m}Tc(CO)_3$-DTMA-(β-Ala)-BBN(7–14)$NH_2]^+$ conjugate in PC-3 tumorbearing mice at 1, 4 and 24 h p.i. (*n*=5,%ID/g±S.D.)

Tissue/organ	1 h	4 h	24 h
Bladder	0.94 (1.25)	0.29 (0.22)	0.00 (0.00)
Heart	0.28 (0.04)	0.18 (0.02)	0.16 (0.31)
Lungs	0.56 (0.07)	0.29 (0.07)	0.10 (0.12)
Liver	5.38 (1.30)	1.99 (0.40)	0.64 (0.19)
Kidney	3.05 (0.51)	1.92 (0.76)	0.48 (0.20)
Spleen	0.38 (0.10)	0.43 (0.19)	0.26 (0.27)
Stomach	0.93 (0.65)	0.39 (0.19)	1.96 (4.08)
Small intestine	25.36 (4.73)	2.19 (1.00)	0.85 (0.93)
Large intestine	1.75 (0.63)	50.63 (27.45)	2.08 (3.62)
Muscle	0.16 (0.03)	0.06 (0.01)	0.02 (0.03)
Bone	0.24 (0.07)	0.13 (0.06)	0.00 (0.00)
Brain	0.03 (0.00)	0.03 (0.01)	0.00 (0.01)
Pancreas	8.20 (2.38)	8.27 (2.47)	4.12 (1.23)
Tumor 1	0.92 (0.17)	0.47 (0.11)	0.11 (0.07)
Tumor 2	0.98 (0.12)	0.56 (0.09)	0.14 (0.07)
Blood	0.73 (0.60)	0.37 (0.24)	0.11 (0.04)
Urine	50.50 (3.07)	57.64 (10.44)	94.01 (5.04)